Electrical transport properties of mono- and polycrystalline $FeWO_4$

1991 J. Phys.: Condens. Matter 3 5341

(http://iopscience.iop.org/0953-8984/3/28/009)

J. Phys.: Condens. Matter 3 (1991) 5341–5352. Printed in the UK

Electrical transport properties of mono- and polycrystalline $FeWO_4$

E Schmidbauer, U Schanz and F J Yu†
Institut fur Allgemeine und Angewandte Geophysik der Universität München, Federal Republic of Germany

Received 21 January 1991

Abstract. The electrical resistivity and thermopower have been measured on semiconducting mono- and polycrystalline $FeWO_4$ between ≈ 100 K and ≈ 1000 K. The DC resistivity ρ, with activation energies $E_A \approx 0.15$–0.32 eV and ρ (294 K) $\approx 5 \times 10^2$–10^5 Ω cm, is probably governed by polaron hopping processes. From thermopower data, p-type conduction is concluded. Non-stoichiometric samples, produced under slightly oxidizing conditions exhibit reduced ρ that appears to be related to the presence of an enhanced content of Fe^{3+} besides Fe^{2+}. AC resistivity $\rho(\nu)$ results of some samples in the frequency range $\nu = 0.5$–50 MHz show a rather weak ν dependence.

1. Introduction

$FeWO_4$ (ferberite) is an end member of the wolframite solid solution series $FeWO_4$–$MnWO_4$. Compositions of this series crystallize in the monoclinic (pseudo-rhombic) wolframite lattice (space group P2/c). Wolframites are an important tungsten ore. Fe–W oxides of this and of similar crystal structures are being analysed for their possible application as anodes in photoelectrolysis [1, 2].

The wolframite structure is characterized by zig-zag chains of edge-sharing MeO_6 octahedra (M = Fe, W) along the [001] direction. There is ordering of Fe and W cations, with each chain being occupied either by Fe or W. Layers of FeO_6 octahedra alternate with those of WO_6 along [100] in the sequence FeWFeW . . . (figure 1). The lattice parameters of natural $FeWO_4$, slightly contaminated by Mn and Mg, are

$a = 4.730$ Å $\quad b = 5.703$ Å $\quad c = 4.952$ Å $\quad \beta = 90°$ [4]

$a = 4.750$ Å $\quad b = 5.720$ Å $\quad c = 4.970$ Å $\quad \beta = 90°10'$ [5].

For polycrystalline synthetic samples, parameters were obtained lying intermediate between those of both data sets [2].

$Fe^{2+}W^{6+}O_4$ is semiconducting and for monocrystalline samples an electrical resistivity $\rho \approx 100$ Ω cm and activation energy $E_A = 0.16$ eV were measured at room temperature [2]; it was concluded that the low ρ is related to the presence of a small amount of Fe^{3+} and that conduction may occur by electron hopping along chains in the [001]

† Present address: Shanghai Institute of Technical Physics, Academia Sinica, Shanghai, People's Republic of China.

0953-8984/91/285341 + 12 $03.50

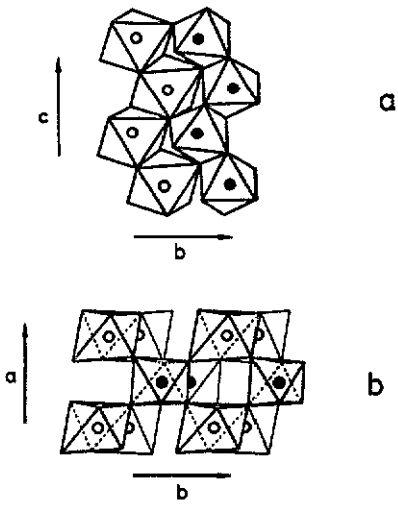

Figure 1. Structural features of the pseudorhombic wolframite crystal structure. (a) Ordering of octahedrally coordinated Fe and W cations in zig-zag chains along the [001] direction; (b) projection on the (001) plane shows layers of Fe and W cations in the sequence FeWFeW . . . along [100] (after [3]).

direction of the lattice. The small increase in ρ for monocrystalline solid solutions $Fe_{1-x}Mn_xWO_4$ relative to $FeWO_4$ was explained by the authors assuming that, evidently, Mn^{2+} do not appreciably block the electron hopping paths; hence, electron transfer may also take place between chains. The charge transport in natural monocrystalline $(Fe_{0.614}Mn_{0.386})WO_4$ between 90 K and 850 K was interpreted as a hopping process, dominated by impurities at low temperatures, and as being intrinsic at high temperatures; a reduced anisotropy was noted in the (010) plane [6]. For polycrystalline $FeWO_4$, ρ (294 K) $\approx$ 150 Ω cm was observed [7].

In this context it appears to be useful to have a look at the conduction mechanisms in other $Me^{2+}WO_4$ oxides in which Fe^{2+} has been replaced completely by $Me^{2+} = Mn^{2+}$, Ni^{2+} or Co^{2+}, because there might be analogies. In monocrystalline $MnWO_4$, small polaron hopping appears to dominate the charge transport in the temperture range 300–600 K, whereas for 600–1200 K a large polaron band conduction model is possibly applicable [8]; essentially the same result has been inferred from conductivity results for a pressed powder of $MnWO_4$ [9]. For pressed $NiWO_4$ powder samples, conductivity data recorded between $\approx$500 K and 1000 K have been described by band theory; however, in the high temperature range, small polaron hopping may occur [10] in addition. The charge transport in pressed $CoWO_4$ powder from 350 K to 900 K has been ascribed to two competing processes: band conduction prevailing at high temperatures and a charge hopping mechanism dominating at low temperatures [11].

We have studied electrical transport properties of mono- and polycrystalline $FeWO_4$ at various tempertures by measuring the electrical resistivity and thermoelectric power.

2. Sample preparation and experimental apparatus

2.1. Single crystals

$FeWO_4$ single crystals were grown by the vapour transport technique from polycrystalline $FeWO_4$ (see below) in the temperature range 900–1000 °C, using $TeCl_4$ as the transport agent. The conditions employed were analogous to those applied in [2]. A

more detailed description of the method and of the grown crystals will be given elsewhere [12]. Samples were subjected to heat treatment in an atmosphere with oxygen partial pressures $p_{O_2} = 10^{-4.4}$ atm. (CO_2 gas) and $10^{-11.6}$ atm. (H_2/CO_2 gas mixture) at 1100 °C for 12 h. The high p_{O_2} was applied in order to test the effect of the presence of a low percentage of Fe^{3+}, introduced during slight oxidation, on the electrical conduction of $FeWO_4$. Cooling conditions were identical to those applied for polycrystalline samples (see below).

Platelets of approximate dimensions $3 \times 0.8 \times 0.3\,mm^3$ were used for electrical measurements. X-ray Laue patterns of the samples showed them to be single crystals. It turned out that the long axis was along [001] and the sample plane was a (100) plane. Part of samples were crushed and used for x-ray powder diffraction analysis (Debye–Scherrer photographs, Co-K_α-radiation, graphite monochromator); they were found to have single-phase wolframite structure. No Te contamination could be detected by electron microprobe analysis; this result suggests a Te concentration in $FeWO_4$ of less than 100 ppm. In addition, any deviation of the ratio Fe/W from unity is less than 1%.

2.2. *Polycrystalline samples*

Samples were prepared by use of the ceramic method, starting from α-Fe_2O_3 (99.995%) and WO_3 (99.999%) powders. Pressed pellets of adequate mixtures were sintered at 900 °C for ≈20 h and, after crushing and repressing, for a second time at 1100 °C in well defined H_2/CO_2 atmospheres. Two different conditions were selected that were identical to those employed for the treatment of single crystals, namely heating at 1100 °C in oxygen partial pressures of (i) $p_{O_2} = 10^{-4.4}$ atm. or (ii) $p_{O_2} = 10^{-11.6}$ atm.; the high p_{O_2} was applied to test the effect of Fe^{3+} on electrical conduction as in the case of single crystals. After termination of sintering, the furnace was switched off and the samples cooled slowly to room temperature at a rate of ≈300 °C h^{-1} from high temperatures to 600 °C and at a lower rate in the temperature interval ≤600 °C. During the cooling period, for low p_{O_2} samples the mixture of the H_2/CO_2 gas flow, used at 1100 °C, was kept constant, whereas high p_{O_2} samples cooled down in CO_2 gas.

For electrical measurements, samples with rectangular cross sections were cut from the pellets; typical sample dimensions were $3 \times 3 \times 4\,mm^3$.

All samples used for electrical measurements were subjected to x-ray analysis; only samples exhibiting a single-phase wolframite structure were taken for experiments. From light microscopic analyses, for sintered samples porosities were found to be in the range $p = 0.2$–0.3, and crystallite sizes of 10–20 μm.

^{57}Fe Mössbauer spectra of polycrystalline low, and high-p_{O_2} samples at 294 K are doublets. For the former they could be fitted adequately to quadrupole doublets with quadrupole splitting QS = 1.53 mm s^{-1} and isomer shift IS = 1.11 mm s^{-1} (relative to a metallic Fe absorber) due to Fe^{2+} in agreement with literature data [13]. For a high-p_{O_2} sample, apart from a Fe^{2+} doublet, a second weak component was detected that doubtless arises from Fe^{3+}; the intensity of this doublet was too low for a reliable fit to be made. In high-p_{O_2} samples we estimate the ratio Fe^{3+}/Fe^{2+} to be <5%.

2.3. *Experiment*

The electrical resistivity of all samples was measured using DC and AC methods; DC resistivities were determined in the temperature range ≈80 K–≈1000 K by means of a Wheatstone bridge, AC resistivities (0.5–50 MHz) in the temperature range 293 K–

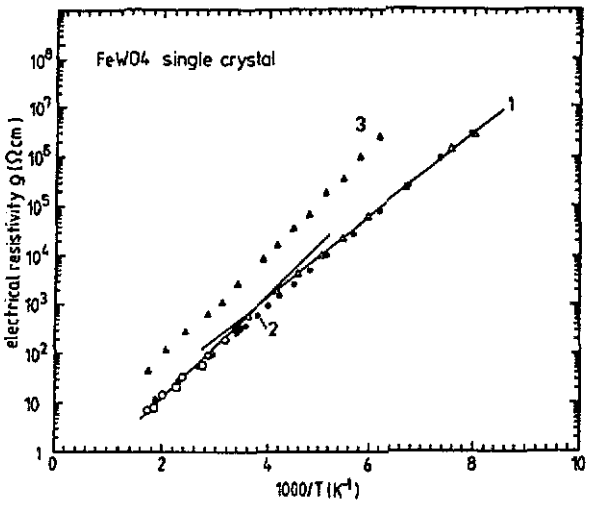

Figure 2. Logarithm of the electrical DC resistivity ρ versus $1/T$ for a $FeWO_4$ single-crystal sample. (1) Original sample; (2) sample annealed at 1100 °C in $p_{O_2} = 10^{-4.4}$ atm.; (3) sample annealed at 1100 °C in $p_{O_2} = 10^{-11.6}$ atm.

≈900 K were measured applying a Schering-type bridge (Hewlett Packard 250 RX meter) and a mini-furnace. In both cases a two-probe method was used. In addition, the thermoelectric power θ was determined from 80 K–≈1000 K, utilizing temperature differences between sample electrodes of 15–20 K. Temperatures were measured at contacts between the sample and Pt-foil electrodes using chromel–alumel thermocouples. Temperature differences ΔT, between sample electrodes were generated by a current through some windings of heating wire close to one Pt electrode; ΔT was determined to ±0.3 K. The error on θ is estimated to be ±10%.

Electrical contacts were provided by a Pt paste (Demetron 308A) rubbed on the clean sample surfaces. Contacted single-crystal and polycrystalline samples were pressed between spring loaded Pt-foil electrodes. To protect samples from being oxidized during measurements at higher temperatures, a stream of N_2 gas (99.999%) was bubbled through the gas-tight Al_2O_3 tube containing the sample holder inside a furnace.

The electrical resistivity and thermopower of monocrystalline samples were measured along [001].

3. Results

3.1. DC resistivity

Figure 2 shows the logarithm of electrical DC resistivity ρ as a function of $1000/T$ for a monocrystalline $FeWO_4$ sample. Curve 1 (empty symbols) stem from the original sample, whereas 2 and 3 are due to samples treated at different oxygen partial pressures p_{O_2}. All curves were reversible when measured several times. We approximate curve 1 by two straight lines of slightly different slopes; there is a break visible somewhat below

Table 1. Parameters deduced from the logarithm of electrical DC resistivity log ρ versus reciprocal temperature $1/T$ for monocrystalline and polycrystalline $FeWO_4$ (figures 2 and 3): E_A = activation energy, ρ_0 = resistivity extrapolated towards $1/T \rightarrow 0$, p_{O_2} = oxygen partial pressure applied during heat treatment or preparation (see section 2).

Sample		ρ_0 (Ω cm)	E_A (eV)
Single crystal			
Untreated	low T	0.75	0.16
	high T	0.13	0.20
Annealed			
At high p_{O_2}		0.25	0.18
At low p_{O_2}		0.77	0.21
Polycrystal			
High p_{O_2}	low T	2.2	0.17
	high T	0.55	0.22
Low p_{O_2}			
Heating	first	1.8	0.32
	second	3.9	0.24
	third	11	0.15

room temperature; on the contrary, curves 2 and 3 can be described by straight lines in the whole temperature range. The straight lines follow the relation for semiconductors

$$\rho = \rho_0 \exp(E_A/kT) \tag{1}$$

with E_A = activation energy, kT = thermal energy. Values for E_A and ρ_0 are listed in table 1. For all curves, E_A is in the range $E_A \approx 0.16$ eV and 0.21 eV, in fair agreement with data from the literature [2]. For low p_{O_2} (1100 °C), ρ at a fixed T is about a factor 5–10 larger than for heating at high p_{O_2}. The low p_{O_2} is expected to be close to the equilibrium p_{O_2} and should result in rather pure $FeWO_4$, whereas for high p_{O_2} a notable concentration of Fe^{3+} must be assumed to be present and, for charge compensation, probably of cation vacancies, □. We suspect that the lowered ρ for high p_{O_2} may be related to the coexistence of neighbouring Fe^{2+} and Fe^{3+} that are known to give rise to electron hopping in many ferrites [14]. As mentioned, the low ρ (294 K) of monocrystalline $FeWO_4$ has been interpreted by this effect [2]. The exact equilibrium p_{O_2} at 1100 °C does not appear to be known. A break in the log ρ–$1/T$ curve, as for the untreated $FeWO_4$ single-crystal sample, suggests the existence of two charge conduction mechanisms with slightly different activation energies E_A.

Analogous curves are presented in figure 3 for polycrystalline samples. For the high p_{O_2} sample, no change in $\rho(T)$ has been noted when multiple measurements were made up to ≈1000 K. The curve can be considered as a superposition of two straight lines with a break at ≈294 K as found for the untreated single crystal (figure 2). The data extracted are listed in table 1. The low p_{O_2} sample shows a variation in the behaviour of $\rho(T)$ after heating to ≈1000 K during measurement; a second and further runs resulted in considerable reduction in ρ at lower T (curves a, b, c). Hence, obviously physico-chemical effects took place that may be related to grain boundary processes or changes in the

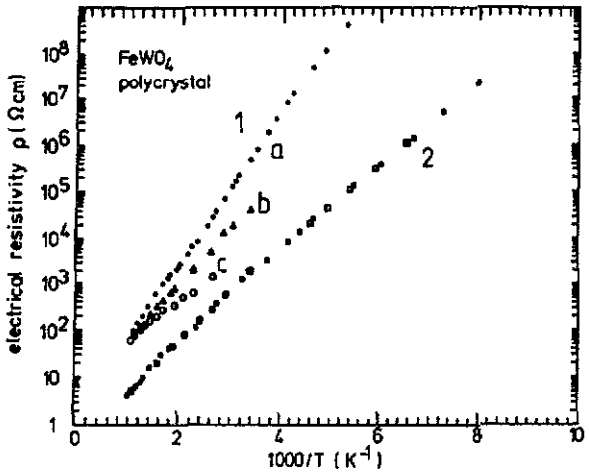

Figure 3. Logarithm of the electrical DC resistivity ρ versus $1/T$ for polycrystalline $FeWO_4$. (1) Sample sintered at 1100 °C in $p_{O_2} = 10^{-11.6}$ atm., (a) first, (b) second, (c) third measuring cycle; (2) sample sintered at 1100 °C in $p_{O_2} = 10^{-4.4}$ atm., different symbols for heating and cooling cycles during measurement.

grain interior. Most probably the alterations are related to oxidation processes where Fe^{3+} and □ are involved.

The $\rho(T)$ values of polycrystalline and monocrystalline samples become nearly parallel for high-p_{O_2} treatment (table 1). ρ (294 K) for polycrystalline samples is only twice as high as that for single crystals. This result shows that there are probably no disturbing effects due to grain boundary layers. The slightly steeper slope in the log ρ–$10^3/T$ curve of the polycrystal above ≈300 K, is hardly detectable for the single-crystal sample; the behaviour resembles that for the untreated single crystal. It should be noted that the maximum applied T for polycrystalline samples during measurement was much higher than for single crystals. A rather large difference in ρ for both kinds of samples is noted in the case of low-p_{O_2} samples, which is due to the enhanced activation energy for polycrystals (table 1). We found that for polycrystalline low-p_{O_2} samples, cooled to room temperature after termination of preparation at varying cooling rates, ρ (294 K) varied up to factor of ≈3. Considering the above facts, it is highly probable that, for polycrystalline low p_{O_2} samples, grain boundary effects play a part in conduction under various conditions.

3.2. AC resistivity

For single-crystal samples, the real part of the AC resistivity Re $\rho(\nu)$ (ν = frequency) can give information on the volume charge transport mechanism. For polycrystals, Re $\rho(\nu)$ is in general used to test whether grain boundaries form layers of increased resistivity, because they are short circuited at high ν [15].

Results of Re $\rho(\nu)$, presented in figure 4 for a single-crystal and polycrystal sample, show a rather small variation of Re $\rho(\nu)$ relative to DC resistivities. Hence, no marked impeding grain-boundary effects are visible for the sintered relative to the single-crystal sample.

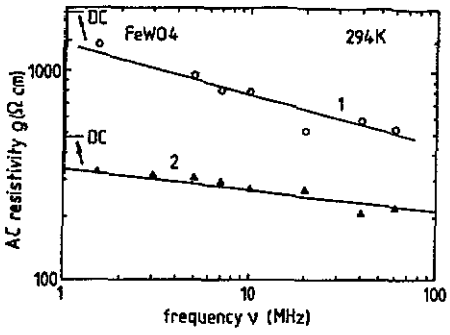

Figure 4. Variation of the real part of the AC resistivity with frequency ν at 294 K for monocrystalline and polycrystalline $FeWO_4$. (1) Polycrystalline sample sintered at 1100 °C in $p_{O_2} = 10^{-4.4}$ atm.; (2) single crystal, untreated.

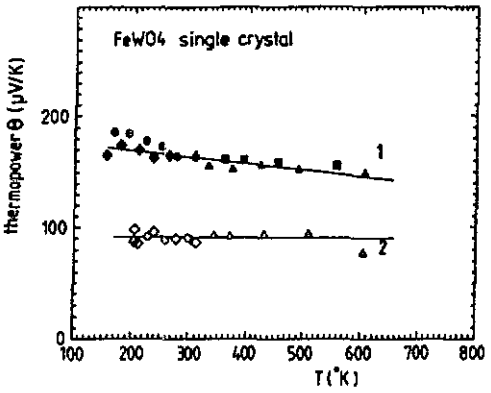

Figure 5. Thermopower θ for monocrystalline $FeWO_4$ as a function of temperature T. (1) Sample annealed at 1100 °C in $p_{O_2} = 10^{-4.4}$ atm.; (2) sample annealed at 1100 °C in $p_{O_2} = 10^{-11.6}$ atm.

Activation energies, E_A, deduced from the T-dependence of Re $\rho(\nu)$ for the samples of figure 4, with $\nu = 1$ and 10 MHz do not notably differ from DC resistivity data.

3.3. Thermoelectric power

Data on thermoelectric power θ versus T for single-crystal samples are illustrated in figure 5. There is a slight roughly linear decrease of θ with rising T for untreated and high-p_{O_2} samples, whereas θ is constant for low-p_{O_2} samples within the accuracy of measurement. The untreated crystal gives θ data in agreement with those for the high-p_{O_2} sample.

The positive sign of θ indicates that $FeWO_4$ is p-type semiconducting and the majority charge carriers are holes. A temperature independent θ, as that of curve 2, is well known for transition metal oxides in which a fixed concentration of charge carriers is present and $\rho(T)$ is dictated completely by the T dependence of the charge carrier drift mobility. In this event, a small polaron charge hopping model is applicable in the whole temperature range [16, 17]. For band conduction, θ is expected to vary notably with T [18]. Curve 1 shows a very reduced T variation, but in a first approximation, we neglect this T effect.

θ values of sintered samples show qualitatively the same behaviour as single crystals. In figure 6(a), typical results are presented for samples sintered at high p_{O_2}. Hollow symbols denote data points recorded during measurements up to ≈600 K; these values agree more or less with those found for single-crystal samples apart from a steeper slope. Full circles represent data points taken during a subsequent measurement up to ≈1000 °C. An analogous situation is evident from figure 6(b) where θ values are displayed for samples sintered at low p_{O_2}. The empty symbols of curve 1 represent points taken at lower temperatures and during the first heating up to ≈850 K; full circles of curve 2 are values during second heating. Obviously, some kind of alteration must have occurred in the sample that resulted in a changed conduction mechanism as was also

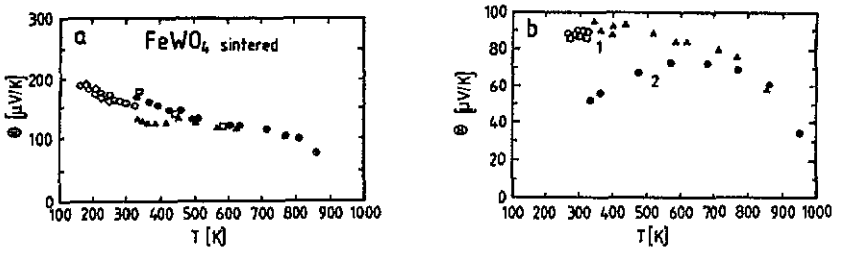

Figure 6. Thermopower, θ, for polycrystalline $FeWO_4$ as a function of temperature T. (a) Sample sintered at 1100 °C in $p_{O_2} = 10^{-4.4}$ atm.; data denoted by symbols $\Delta\Delta\Delta$ are recorded after the high-T run. (b) Sample sintered at 1100 °C in $p_{O_2} = 10^{-11.6}$ atm.; first run up to high-T denoted by symbols $\Delta\Delta\Delta$, second run by ●●●.

concluded from ρ data. As in the case of ρ (294 K), θ (294 K) of polycrystalline low-p_{O_2} samples varied, depending on the cooling conditions after termination of preparation. Thus, it was noticed that faster cooling than used for the samples under study shifted θ (294 K) from $\approx +90\,\mu V\,K^{-1}$ (figure 6) to $\approx +140\,\mu V\,K^{-1}$ but no particular change in the T dependence was established.

4. Discussion

4.1. DC resistivity

In 3d transition metal oxides, 2s and 2p oxygen orbitals overlap strongly with 4s and 4p orbitals of transition metal ions. The top of the full broad oxygen 2p band is in general separated by an energy band gap of several eV from 4s and 4p bands [18, 19]. Due to reduced orbital overlapping of 3d transition metal cations, there are narrow 3d bands in the energy gap which may also be valid for Fe^{2+} in $FeWO_4$. In an octahedral environment, degenerate 3d orbitals split under the action of the crystal field in lower triplet t_{2g} and higher doublet e_g levels which are in fact narrow subbands. Due to electron correlation effects, possibly t_{2g} and e_g bands are, in addition, further subdivided into spin up $\uparrow$ and spin down $\downarrow$ subbands [19]. In any case, the subbands must be either full or empty in order to get semiconducting properties. The position of subbands and the behaviour of charge carriers in this model appears to be far from being understood to date; this is valid even for the simple binary oxides NiO, CoO, MnO [20–23]. For $FeWO_4$, the empty 5d W^{6+} band is expected to lie above the Fermi level which must be above the full Fe^{2+} 3d subbands.

In polar crystals, due to strong electron–lattice coupling, polaron conduction determines electrical properties in narrow band semiconductors. In the case of strong coupling, according to theory, band conduction may occur at low T, whereas at high T the band model can break down if $T > \theta/2$ (θ = Debye temperature) and phonon assisted polaron hopping between neighbouring cations can occur when the coupling exceeds a critical strength (non-adiabatic case) (see for reviews [16–18]). Such behaviour is accompanied by low drift mobility μ_D of charge carriers.

For semiconducting materials with low μ_D ($\mu_D < 0.1\ cm^2\ V^{-1}\ s^{-1}$) a relation for the electrical conductivity σ of

$$\sigma = CT^{-3/2} \exp(-E_A/kT) \tag{2}$$

with C = constant, has been derived for small polaron hopping (non-adiabatic case); a factor T^{-1} is present in the preexponential factor for the adiabatic case [18, 19].

Neighbouring cations of the same kind but differing valencies (Me^{n+}, $Me^{(n+1)+}$) on equivalent lattice positions in oxides have been found to enable localized electron (polaron) hopping between both kinds of cations. This mechanism of charge transfer plays an essential role in many transition metal oxides [14, 24]. In $FeWO_4$, it may concern Fe^{2+} and a small amount of Fe^{3+}, as mentioned. Such a model is in agreement with the positive thermopower that indicates p-type conduction. There remains the question as to whether in pure $FeWO_4$ tiny concentrations of Fe^{3+} and W^{5+} are present in equal parts that would probably affect conduction. A certain small content of Fe^{3+} (and □) may be introduced by sample treatment at high T in a slightly oxidizing atmosphere as mentioned; after cooling, Fe^{3+} and □ are frozen in. To create one □, two Fe^{2+} have to be converted into Fe^{3+}, hence a configuration Fe^{3+}–□–Fe^{3+} represents a neutral □. Small polaron hopping may occur by electron transfer from Fe^{2+} to neighbouring Fe^{3+}. The detailed role of □ is not known; it depends doubtless on the type of related lattice defects. There may be Fe^{3+}–□–Fe^{3+} clusters which possibly form in Fe zig-zag chains along [001]. These clusters may arise because of the requirement of local charge balance. The presence of □ may mean a termination of one-dimensional charge transport between neighbouring Fe^{2+} and Fe^{3+}. Also, singly and doubly ionized □ may exist; in addition, interstitial Fe^{3+} can be imagined. For enhanced concentrations of Fe^{3+} (and □), interaction of the above defects may also take place, giving rise to more complex clusters. All arrangements of Fe^{3+} and □ represent disorder in $FeWO_4$. In addition, incomplete ordering of Fe and W in the lattice may play a part. The exact type of charge hopping depends on the structure and number of defects.

The electrical conductivity σ is described for a single kind of charge carriers by

$$\sigma = ne\mu_d \tag{3}$$

with σ = electrical conductivity, n = concentration of charge carriers, e = electronic charge and μ_d = drift mobility. In general, in low mobility materials with $\mu_d < 0.1\ cm^2\ V^{-1}\ s^{-1}$, it is suggested that small polaron hopping takes place [16].

Our ρ data for monocrystalline samples, heated at high and low p_{O_2} (figure 2), point to a semiconducting charge mechanism between 160 K and ≈600 K with activation energies $E_A \approx 0.18$ and 0.21 eV, respectively. These data are compatible with an $Fe^{2+} \rightarrow Fe^{3+}$ electron hopping model. A strong effect of Fe^{3+} on conduction has been ascertained for high-p_{O_2} samples. Hence, we try to explain the charge transport in terms of some kind of $Fe^{2+} \rightarrow Fe^{3+}$ hopping. Band properties may be effective at higher T as used. As mentioned above, a further point to be considered here is imperfect ordering of Fe and W in chains (see section 1); it may effect $Fe^{2+} \rightarrow Fe^{3+}$ hopping processes. Although such an effect has not been studied it appears probable, in particular for samples treated at the rather large T = 1100 °C (melting point ≈ 1250 °C). Such a situation raises the question of charge transport between neighbouring chains of cations departing from a mere conduction along Fe chains.

4.2. AC resistivity

Whereas DC conductivity means complete percolation between sample electrodes, AC conductivity includes limited paths. For hopping conductivity, the paths become shorter

in terms of the number of hops as frequency increases. In a large number of disordered semiconductors, the electrical AC conductivity $\sigma(\omega)$, defined as $\sigma(\omega) = \mathrm{Re}\,\sigma(\omega) - \sigma_{DC}$, has been found to vary with angular frequency ω in the hopping region as

$$\sigma(\omega) = \text{constant}\ \omega^n \tag{4}$$

with $n = 0.5$–1 [25, 26]. From theory, this relation should hold for pair hopping processes [25]. Our experimental n (figure 4) is much lower than that found in the literature data presented in [26], with $n \approx 0.1$–0.2. This result may mean that multiple hopping mechanisms occur. A detailed charge hopping model is not available at present.

4.3. Thermopower

The θ data are nearly constant in a large T range. In this event, a formula may be used that has been derived for small polaron hopping [27]

$$\theta = +\,(k/e)[\ln \beta n/(N-n) + C] \tag{5}$$

with β = spin degeneracy factor, n = number of charge carriers, N = number of available sites and C = entropy term. For $n < N/2$ and $\beta = 1$, θ is negative; and for $N/2 < n < 1$, θ is positive. Anticipating that charge transport in $FeWO_4$ is effected predominantly by polaron hopping of the type $Fe_i^{2+} + Fe_j^{3+} \rightarrow Fe_i^{3+} + Fe_j^{2+}$, then n = number of Fe^{2+} that provide electrons for the hopping process, N = number of $Fe^{2+} + Fe^{3+}$. We expect a reduced positive θ for increased concentrations of Fe^{3+}, i.e. for high-p_{O_2} relative to low-p_{O_2} samples (figure 5). We adopt the belief that all Fe sites (1/2 of occupied cation sites) are available for electron exchange along [001] and that the concentration of Fe^{3+} is low compared with that for Fe^{2+}. From the experimental θ, the ratio $(N-n)/n = Fe^{3+}/Fe^{2+}$ can be calculated; for this, the entropy term C in (4), which is assumed to be low, is neglected and β is taken to be 1. This follows for monocrystalline low-p_{O_2} samples $Fe^{3+}/Fe^{2+} \approx 0.37$, in the case of high-$p_{O_2}$ it is ≈ 0.14; for $\beta = 2$, both values have to be multiplied by two. The numbers are probably:

(i) by far too large since only a low concentration of Fe^{3+} is expected to be present,
(ii) in contrast to expectation that Fe^{3+} concentration is enhanced for high p_{O_2}.

Thus, the above simple picture does not appear to apply here.

It seems as if only part of Fe^{2+} is available for electron hopping; i.e. n in (5) is lower than suggested. The above concept may apply preferentially for low-p_{O_2} samples where, due to the low concentration, Fe^{3+} ions do not interact with each other. Hence, some of the Fe^{2+} do not appear to offer an electron for the hopping process to a neighbouring Fe^{3+}, possibly because their electron is jammed between Fe^{3+} and □ or W by some mechanism.

We suspect that for high-p_{O_2} samples, with enhanced Fe^{3+} content, possibly Fe^{3+}–□ cluster arrangement (as is well known from $Fe_{1-\delta}O$ [28]) or that interstitial Fe^{3+} may occur, hence an additional effect comes into play. Both effects may act in reducing the offer of Fe^{2+} electrons for conduction. Furthermore, in both cases it is easily conceivable that the activation energies deduced from $\rho(T)$ curves differ from those for low p_{O_2} samples, since the charge hopping processes differ.

In order to explain the conductivity data for $MnWO_4$, measured perpendicularly to [001], a $Mn^{2+} \rightarrow Mn^{3+}$ electron transfer process was proposed including the presence of □ [8]. From the temperature-dependent θ data, an energy-band model was inferred in a large T range which does not appear to be applicable for our monocrystalline $FeWO_4$.

The θ data for polycrystalline $FeWO_4$ high-p_{O_2} samples show a stronger T dependence than single crystals (figure 5), whereas the low-p_{O_2} samples reveal an almost T independent θ below ≈ 700 K, in agreement with single crystals. However, after heating up to ≈ 1000 K during the measurements, low-p_{O_2} samples change their behaviour obviously and T dependence of θ becomes evident. This change is consistent with an altered ρ (figure 3) and it is probably related to some structural variation. A detailed explanation of this result cannot be given at the moment. Anisotropic conduction may possibly play a role, since for single crystals the conductivity parameters were measured along [001], whereas for polycrystals different conduction paths are conceivable. For high-p_{O_2} samples it could well be that in sintered material more Fe^{3+} are present than in monocrystalline samples because equilibrium may have been attained during sintering, whereas single crystals, treated under the same conditions for ≈ 12 h, may not have been equilibrated, and the Fe^{3+} concentration may have been lower. In both cases, however, the magnitude of θ does not differ much in contrast to expectation. Also, both kinds of high-p_{O_2} samples have very similar activation energies, E_A, for resistivity (table 1).

In conclusion, it can be established that for polycrystalline low-p_{O_2} samples the charge transport parameters studied show a notable variation with preparation conditions.

Acknowledgments

The authors are indebted to Dr W Steurer, Institut fur Kristallographie und Mineralogie, Universität München, for determining the orientation of single-crystal samples and to Dr Th Kunzmann, Petrographisch-Mineralogisches Institut, Universität München, for electron microprobe analysis. This study was supported by a grant from Deutsche Forschungsgemeinschaft.

References

[1] Leiva H, Dwight K and Wold A 1982 *J. Solid State Chem.* **42** 41
[2] Sieber K, Leiva H, Kourtakis K, Kershaw R, Dwight K and Wold A 1983 *J. Solid State Chem.* **47** 361
[3] Kihlborg L and Gebert E 1970 *Acta Crystallogr.* B **26** 1020
[4] Ülkü D 1967 *Z. Kristallogr.* **124** 192
[5] Cid-Dresdner H and Escobar C 1968 *Z. Kristallogr.* **127** 61
[6] Guha Thakurta S R and Dutta A K 1980 *Bull. Minéral.* **103** 27
[7] Noda Y, Shimada M, Koizumi M and Kanamura F 1979 *J. Solid State Chem.* **28** 379
[8] Bharati R, Singh R A and Wanklyn B M 1982 *J. Phys. Chem. Solids* **43** 641
[9] Dissanayake M A K L, Ileperuma O A and Dharmasena P A G D 1989 *J. Phys. Chem. Solids* **50** 359
[10] Bharati R, Singh R A and Wanklyn B M 1980 *J. Mater. Science* **15** 1293
[11] Yadav R B 1983 *J. Phys. Chem. Solids* **44** 697
[12] Yu F J, Schanz U and Schmidbauer E unpublished
[13] Grandjean F and Gérard A 1982 *Valence instabilities* ed P Wachter and H Boppart (Amsterdam: North-Holland) p 587
[14] Klinger M I and Samokhvalov A A 1977 *Phys. Status Solidi* b **79** 9
[15] Koops C G 1951 *Phys. Rev.* **83** 121
[16] Austin I G and Mott N F 1969 *Adv. Phys.* **18** 41
[17] Böttger H and Bryksin V V 1985 *Hopping conduction in solids* (Weinheim: VCH Verlagsgesellschaft)
[18] Adler D 1968 *Solid State Phys.* vol 21, ed F Seitz, B Turnbull and H Ehrenreich (New York: Academic) p 1
[19] Bosman A J and van Daal H J 1970 *Adv. Phys.* **19** 1

[20] Brandow B H 1977 *Adv. Phys.* **26** 651
[21] Hugel J and Carabatos C 1983 *J. Phys. C: Solid State Phys.* **16** 6713
[22] Terakura K, Oguchi T, Williams A R and Kübler J 1984 *Phys. Rev.* B **30** 4734
[23] Mochizuki S 1988 *J. Phys. C: Solid State Phys.* **21** 5183
[24] Jonker G H and van Houten S 1961 *Halbleiterprobleme* **6** 118
[25] Pollak M and Geballe T H 1961 *Phys. Rev.* **122** 1742
[26] Hill R M and Jonscher A K 1977 *J. Non-Cryst. Solids* **32** 53
[27] Chaikin P M and Beni G 1976 *Phys. Rev.* B **13** 647
[28] Garstein E, Cohen J B and Mason T O 1986 *J. Phys. Chem. Solids* **47** 774